

Neutrino-mass determination from tritium β decay: Corrections to and prospects of experimental verification of the final-state spectrum

Svante Jonsell,¹ Alejandro Saenz,² and Piotr Froelich¹

¹*Institute for Theoretical Atomic and Molecular Physics, Harvard-Smithsonian Center for Astrophysics, 60 Garden Street, Cambridge, Massachusetts 02138*

and Department of Quantum Chemistry, Uppsala University, Box 518, S-751 20 Uppsala, Sweden

²*Max-Planck-Institute for Quantum Optics, Hans-Kopfermann-Straße 1, D-85748 Garching, Germany*

(Received 25 February 1999; published 26 July 1999)

We have investigated the final-state spectrum of HeT^+ and HeH^+ following β decay of T_2 or TH. For the electronically bound-state part of the spectrum the effects of a corrected recoil, improved potential curves for the excited states, nonadiabatic effects, and excitations of the initial molecular state have been investigated. We also discuss the feasibility of various experimental methods to verify the theoretical final-state spectrum.

[S0556-2813(99)02808-3]

PACS number(s): 31.15.-p, 23.40.Bw, 14.60.Pq

I. INTRODUCTION

The question of the neutrino mass remains one of the outstanding problems of physics. Recent measurements of atmospheric and solar neutrinos indicate that oscillations between the different neutrino flavors do occur, which implies that neutrinos indeed are massive [1]. The most direct method of determining the neutrino mass is, however, the analysis of the shape of β -decay spectra in the energy region close to the maximum of the β -electron energy. The upper bound to the (electron anti-)neutrino mass obtained from this type of experiments is now approaching 1 eV/ c^2 [2,3]. A surprising difficulty in reaching a better sensitivity is the appearance of some unknown systematic effect due to which most of the more recent experiments have obtained a best value for the neutrino mass squared m_ν^2 that lies within the unphysical negative region [2–7].

One complication in the neutrino-mass determination from β -decay spectra is their dependence on the amount of energy released in excitations of the atomic or molecular surroundings. To reduce the complexity of this dependence the experiments were performed with the simplest tritium-containing compound that is experimentally still possible to handle, the T_2 molecule. The full quantum-mechanical treatment of the transition probability is nevertheless a complicated theoretical problem at the level of accuracy needed for the interpretation of the experiments. It is therefore worthwhile to make careful investigations whether the unexpected experimental results may be due to any inaccuracy in the theoretical final-state spectrum.

In a series of papers from the 1980s [8–13] a very careful calculation of the final-state spectrum was presented. More recently several articles have addressed the accuracy of these calculations and made several refinements [14–20]. Most of the more recent refinements within the sudden approximation have focused on the electronic continuum, i.e., the states where one of the molecular electrons acquires enough energy to be exerted from the molecule. These states make up roughly 14% of the final-state probability. The aim of the present paper is to reinvestigate the remaining 86% of the

final-state probability, where both molecular electrons remain bound to the HeT^+ molecular ion, and in particular the electronic ground state which constitutes about 57% of the final-state probability. Such an investigation has become all the more important since recent experimental results [7,3] indicate that the source of the negative m_ν^2 anomaly lies close to the end-point of the β -electron spectrum, i.e., in the energy region most influenced by the low-energy final molecular states. A refined table of the final-state spectrum containing the results of this paper and those of Ref. [19] will be published separately [21].

The refinements of the theoretical calculations discussed in this article include: a relativistic correction to the molecular recoil (caused by the emitted β electron), decay from initially rotationally excited T_2 molecules, nonadiabatic corrections to the Born-Oppenheimer approximation, improved potential energy curves as well as transition matrix elements for the excited states, and isotope effects (assuming an impurity admixture of TH). We will also discuss possible methods of experimental assessment of the accuracy of the final-state spectrum, and review the available experimental results that can be used for this purpose.

II. THE NEUTRINO MASS FROM β DECAY

We consider the β -decay process

$$\text{T}_2 \rightarrow {}^3\text{HeT}^+(f) + e^- + \bar{\nu}_e, \quad (1)$$

where f designates a molecular state of the daughter ion. The conservation of energy and momentum in the reaction (1) leads to a continuous distribution of kinetic energies of the β electron. If the amount of energy released was known with sufficient accuracy, then one could in principle deduce the neutrino mass from the maximum measured energy of the β electron. However, the knowledge of the energy release is limited due to the insufficient accuracy of the nuclear masses involved. In addition, this is not a practical approach since near the end-point energy (i.e., the maximum energy of the β electron) the spectral intensity is very weak, and approaches the background smoothly. Instead one studies the *shape* of

the spectrum near the end-point energy. The intensity $I(E_\beta)$ is a function of the kinetic energy E_β of the β electron, its momentum $p_\beta = \sqrt{E_\beta^2 + 2m_e c^2 E_\beta}/c$, and, most importantly, depends parametrically on the neutrino mass m_ν [12],

$$I(E_\beta) = AF(p_\beta)p_\beta(E_\beta + m_e c^2) \sum_f P_f(K) \times (W_0 - E_f - E_\beta) \Theta(W_0 - E_f - E_\beta - m_\nu c^2) \times \sqrt{(W_0 - E_f - E_\beta)^2 - m_\nu^2 c^4}, \quad (2)$$

$$F(p_\beta) = \frac{2\pi\eta}{1 - \exp(-2\pi\eta)}, \quad (3)$$

$$\eta = m_e e^2 / \hbar p_\beta. \quad (4)$$

Here A is a normalization constant, $F(p_\beta)$ is the so called Fermi function, η the Sommerfeld parameter, W_0 is the maximum kinetic energy of the electron if one would have a vanishing neutrino mass, i.e., $m_\nu = 0$, K the recoil momentum of the molecule, and E_f , P_f , are the energy and probability of the final molecular state f . The Heaviside step function Θ ensures that the intensity is real. The experimental data are fitted to the form (2) with A , W_0 , and m_ν^2 (as well as experimental parameters such as the background) as free parameters. Thus m_ν is neither determined from the absolute strength of the intensity $I(E_\beta)$, nor from the maximum β -electron energy, but manifests itself in the *shape* of the intensity over a range of β -electron energies, i.e., by the quality of the fit. From Eq. (2) one sees that the modification of $I(E_\beta)$ due to a nonvanishing neutrino mass will only be nonnegligible when $m_\nu c^2 \lesssim W_0 - E_f - E_\beta$, i.e., when E_β is close to its maximum value $W_0 - E_f - m_\nu c^2$.

Because of the small value of the neutrino mass, $m_\nu \approx 0$, the statistical fluctuations around this central value will require, in order to be able to perform an experimental χ^2 fit, that the form (2) is extended into the region $m_\nu^2 < 0$. On the other hand, it should be noted that the form (2) is derived under the physical assumption that $m_\nu^2 \geq 0$. Such an extension therefore has no physical content, and is to a certain extent arbitrary. Indeed different extensions have been used by different experimental groups, as discussed in Ref. [16]. A best fit that results in a value of the neutrino mass squared that lies several standard deviations within the $m_\nu^2 < 0$ region therefore has no physical content other than that the experimental results do not agree with the theoretical prediction (2).

Since the fit contains several free parameters, and since the experimental spectrum contains statistical errors, with very complex interdependence, it is very difficult to identify the source for the observed discrepancy between the experimental spectrum and the theoretically predicted form. In particular, since the functional dependence of m_ν^2 relies only on the assumption that Fermi theory for β decay is valid, it is reasonable to search for a discrepancy among the other theoretical or experimental parameters entering the fit. In the Troitsk experiment the source of the anomaly has been identified as a ‘‘bump’’ in the β -electron spectrum very close to

the end point, the inclusion of which in the fit yielded a positive m_ν^2 value [7,3]. The physical cause of this bump has not yet been determined with certainty. Since experiments indicate that close to the end point, $I(E_\beta)$ does not agree with the theoretical prediction in Eq. (2), this turns the attention to the parameters $P_f(K)$ and E_f , and in particular to the molecular states that lie lowest in energy, and thus influence the shape of the β spectrum close to the end point.

The parameters $P_f(K)$ and E_f must be obtained by theoretical calculations. It is evidently important to investigate the accuracy of these parameters both theoretically and by independent measurements. In any theoretical calculation a number of assumptions have to be made. We will, except when we explicitly declare otherwise, assume that the decaying triton is bound in a free T_2 (or TH) molecule, and that the β electron does not undergo any inelastic processes under its way to the analyzer. There is a number of external effects, not accounted for here, which may influence the β spectrum, such as secondary scattering, external electric or magnetic fields, decay of impurities (e.g., of HeT^+ molecules that accumulate as the source ages), and solid-state effects. [A recipe for introducing solid-state effects into a final-state distribution obtained for a free T_2 molecule (as presented, e.g., in this work) has been given in Ref. [13].] Most of these factors are specific to each experiment, and the corresponding statistical uncertainties have been evaluated by the experimental groups. On the theory side we assume the validity of Fermi theory for β decay, the validity of the sudden approximation (which has been analyzed and refined in Ref. [19]), and that nonrelativistic wave functions can be used for the molecule.

III. TRANSITION PROBABILITIES TO ELECTRONICALLY BOUND STATES REVISITED

Let us now turn to the calculation of the final-state energies E_f and probabilities P_f in some more detail. Consider a particular rovibrational state of the ${}^3\text{HeT}^+$ molecule, $f = \{n, \nu, J, M\}$, where n is the electronic state, ν the vibrational quantum number, and J, M are the rotational angular-momentum quantum numbers of the molecule. Assuming the validity of the sudden approximation and ignoring recoil-induced electronic transitions (see [18,19]), and the Born-Oppenheimer approximation (see Ref. [20] and Sec. III D), and that the momentum of the neutrino is much smaller than that of the β electron (which certainly is true near the end-point energy, since even at 1.3 keV below the end-point the momentum of the neutrino is about 1% of the β -electron momentum) the transition probability is given by [12]

$$P_{n\nu JM}(K) = \left| \int [\chi_{\nu JM}^n(\mathbf{R})]^* S_n(R) e^{i\mathbf{K}\cdot\mathbf{R}} \xi_{\nu_i J_i M_i}^{n_i}(\mathbf{R}) d^3R \right|^2. \quad (5)$$

Here $\xi_{\nu_i J_i M_i}^{n_i}$ and $\chi_{\nu JM}^n$ are the usual rovibrational wave functions of the T_2 and the HeT^+ molecule, respectively, $S_n(R)$ is the overlap of the electronic wave function describing the final state n with the initial ground electronic state of T_2 . The exponential arises from the recoil from the emerging β elec-

tron. The recoil momentum is $\mathbf{K} = -M_T / (M_{\text{He}} + M_T + 2m_e) \mathbf{k}_\beta$, where $\mathbf{k}_\beta = \mathbf{p}_\beta / \hbar$. R is the internuclear distance. For the initial ground state $n_i = 1$, $v_i = J_i = M_i = 0$ Eq. (5) reduces to

$$P_{n\nu J}(K) = (2J+1) \left| \int_0^\infty S_n(R) j_J(KR) f_{\nu J}^n(R) g_{00}^1(R) dR \right|^2, \quad (6)$$

where a summation over the rotational quantum number M has been performed. Here $f_{\nu J}^n(R)/R$ is the radial part of $\chi_{\nu JM}^n(\mathbf{R})$, $g_{\nu J_i}^{n_i}(R)/R$ the radial part of $\xi_{\nu J_i M_i}^{n_i}(\mathbf{R})$, and $j_J(R)$ is the spherical Bessel function.

For the electronic energies of T_2 we used the same data and procedure as in Ref. [22]. This includes adiabatic, relativistic and radiative corrections to the Born-Oppenheimer approximation. For the ground state of HeT^+ we used the same data as were used in Ref. [9], namely, the electronic overlap $S_1(R)$ from Ref. [8], Born-Oppenheimer energies from Refs. [23–25], and the adiabatic correction from Ref. [25]. The data in Ref. [23] do, however, start at $R = 0.9$ a.u., which we found insufficient. Therefore we added two points at $R = 0.6$ a.u. and 0.8 a.u. from Ref. [8] and extrapolated the adiabatic correction.

The Born-Oppenheimer energies and the electronic overlaps $S_n(R)$ for the excited states of HeT^+ were calculated using the same method as in the earlier works by Kolos *et al.*, see, e.g., Ref. [8]. This method uses explicitly correlated basis functions in prolate-spheroidal coordinates. By using 400 basis functions and three different sets of nonlinear exponents the potential energy curves and transition probabilities displayed in Table I and Fig. 1 were obtained. The energies in Ref. [8] were used in a few cases when they were lower than ours. However, it may be noted that in the important range of R values, i.e., in the Franck-Condon region of the T_2 ground state, all potential curves obtained in this work are lower than the ones published before. In the calculation of $S_n(R)$ the T_2 ground-state wave function from Ref. [26] was used.

The wave functions of nuclear motion and required R integrals were calculated using adaptations of the programs LEVEL6.0 [27] and BCONT1.4 [28] by Robert Le Roy. Our results for the energies of the rovibrational levels agree with those of Ref. [9] to within 10^{-4} eV. We could also reproduce the transition probabilities in Ref. [9] to within 0.00001. The main reason for the difference in energy is probably that less accurate Born-Oppenheimer energies for T_2 were used in Ref. [9]. The values used for the low R part of the HeT^+ ground state may also be slightly different. Another difference is that we used the 1986 CODATA value of 1 Hartree = 27.21139 eV, while 1 Hartree = 27.2116 eV was used in Ref. [9].

A. Relativistic correction to the recoil

From Eq. (5) we see that the rovibrational excitations depend on the energy of the β electron via the recoil. In Ref. [9] the relation $p_\beta = \sqrt{2m_e E_\beta}$ was used for calculating the recoil momentum. Since the end-point kinetic energy of the

β electron is 4% of its mass, and since it introduces no additional complication, we instead used the relativistic relation $p_\beta = \sqrt{E_\beta^2 + 2m_e c^2 E_\beta} / c$. For β -electron energies near the end-point energy, i.e., $E_\beta = 18.6$ keV, one then finds $K = 18.7a_0^{-1}$, rather than the nonrelativistic result $K = 18.5a_0^{-1}$. This results in an increase of the recoil momentum by about 1%. Since K is large, the Bessel functions in Eq. (6) oscillate rapidly, and even small changes in their argument can give rather large changes in the transition probability. Examples of this are shown in Table II, where it is shown that the probability of certain transitions changes by as much as 40%. However, since a sum rule for the probabilities of all rovibrational levels of a given electronic state remains unchanged by the modified recoil [9],

$$P_n = \sum_{\nu, J} P_{n\nu J} = \int S_n^2(R) [g_{00}^1(R)]^2 dR, \quad (7)$$

all changes in the probability of one rovibrational level must be compensated for by corresponding changes in other levels. We see in Table II that including the correction to the recoil has the effect of moving probability from lower to higher vibrational levels, as one would expect when the recoil momentum increases. In Fig. 2 we observe the same trend for the rotational levels. The resulting probability as a function of energy is shown in the second column of Table III. The relative change of individual bins compared to the results in Ref. [9] is up to about 10%. On a larger scale the changes are however small, since due to the sum rule (7) the total probability P_1 of the ground state remains unchanged, and the mean excitation energy of the ground state $\sum_{\nu, J} P_{1\nu J} E_{1\nu J}$ changes by only 0.03 eV.

The results presented in Tables II, III and Fig. 2 are all for a β -electron energy $E_\beta = 18.6$ keV. As one moves away from this end-point energy the recoil will decrease. However, as noted in Ref. [9] the effect is small as long as the changes to E_β are on the order of 100 eV. In fact at about 300 eV below the end-point energy the decrease in recoil cancels the relativistic correction, and the results in Ref. [9] are regained.

B. Excited initial state

It is usually assumed that the decaying nucleus is bound in a T_2 molecule being in its ground rovibrational state. Whether this assumption is valid depends on the experimental conditions. If the experiment is performed at room temperature a significant fraction of the T_2 molecules are in an excited rotational state. Assuming a Maxwell-Boltzmann distribution at 273 K only about 1/3 of the T_2 atoms will be in the $v=0, J=0$ state. Furthermore at low temperatures the transition from ortho- T_2 to para- T_2 , i.e., from J odd to J even, is slow. After a gas of T_2 is cooled down to low temperatures one would therefore expect a statistical distribution between the $J=0$ and $J=1$ states, i.e., 75% of the molecules in the $J=1$ state and 25% in the $J=0$ state. The rate of the $J=1 \rightarrow J=0$ transition will depend on the experimental conditions. This effect is not present for TH, i.e., there are no long-lived rotationally excited states.

TABLE I. Electronic energies in Hartree (upper value) and the squared overlap integrals $S_n^2(R)$ (lower value) of the excited states 2–6 of HeT^+ . The numbers marked by asterisks were taken from Ref. [8].

R	2	3	4	5	6
0.60	−0.693 247 94 0.043 486	−0.653 023 90 0.103 900	−0.357 422 10 0.000 931	−0.348 755 33 0.007 118	−0.333 100 58 0.025 012
0.80	−1.285 543 86 0.060 842	−1.201 160 10 0.100 865	−0.973 743 68 0.007 258	−0.961 723 85 0.000 074	−0.945 590 65 0.014 186
1.00	−1.609 875 94 0.091 445	−1.475 413 44 0.094 181	−1.277 621 36 0.008 140	−1.259 381 60 0.000 057	−1.237 091 88 0.011 484
1.10	−1.724 412 22 0.109 539	−1.563 071 25 0.090 531	−1.378 233 44 0.008 497	−1.356 588 78 0.000 069	−1.330 750 79 0.010 839
1.20	−1.819 950 73 0.128 693	−1.631 028 53 0.086 720	−1.458 553 59 0.008 594	−1.433 562 32 0.000 084	−1.404 221 26 0.010 308
1.30	−1.901 729 29 0.148 365	−1.685 031 06 0.082 811	−1.524 216 99 0.008 434	−1.496 197 36 0.000 100	−1.463 400 89 0.009 794
1.35	−1.938 546 79 0.158 249	−1.708 062 46 0.080 820	−1.552 798 17 0.008 265	−1.523 427 88 0.000 105	−1.488 908 64 0.009 544
1.40	−1.973 072 85 0.168 136	−1.728 950 58 0.078 801	−1.579 016 04 0.008 053	−1.548 451 71 0.000 111	−1.512 202 51 0.009 360
1.50	−2.036 093 34 0.187 748	−1.765 441 29 0.074 742	−1.625 519 97 0.007 530	−1.592 986 67 0.000 119	−1.553 463 28 0.008 816
1.60	−2.092 167 26 0.207 108	−1.796 356 37 0.070 634	−1.665 584 23 0.006 938	−1.631 656 74 0.000 120	−1.588 835 90 0.008 309
1.80	−2.186 926 17 0.245 248	−1.846 244 27 0.062 397	−1.731 328 46 0.005 708	−1.696 361 48 0.000 100	−1.646 914 53 0.007 335
2.00	−2.262 279 54 0.283 344	−1.885 147 54 0.054 367	−1.783 297 86 0.004 556	−1.749 301 64 0.000 056	−1.693 160 92 0.006 393
2.20	−2.321 600 45 0.322 131	−1.916 554 21 0.046 778	−1.825 589 13 0.003 517	−1.794 174 32 0.000 012	−1.731 150 36 0.005 501
2.40	−2.367 696 62 0.361 775	−1.942 477 63 0.039 771	−1.860 757 69 0.002 571	−1.833 119 86 0.000 004	−1.762 955 48 0.004 688
2.60	−2.403 018 10 0.401 757	−1.964 193 49 0.033 385	−1.890 552 59 0.001 702	−1.867 412 24 0.000 086	−1.789 879 85 0.003 903
2.80	−2.429 657 52 0.441 631	−1.982 582 25 0.027 608	−1.916 368 58 0.000 866	−1.897 687 04 0.000 292	−1.812 798 91 0.003 316
3.00	−2.450 350 0* 0.480 53*	−1.998 807 8* 0.022 49*	−1.940 243 8* 0.000 20*	−1.923 993 9* 0.000 64*	−1.834 218 7* 0.002 73*
4.00	−2.494 049 8* 0.625 62*	−2.062 147 8* 0.001 70*	−2.032 845 2* 0.004 95*	−2.003 562 0* 0.000 06*	−1.908 003 4* 0.000 43*

The analog of Eq. (6) for a rotationally excited initial state $J_i=1$ is

$$P_{nvJ} = (J+1) \left| \int_0^\infty S_n(R) j_{J+1}(KR) f_{vJ}^n(R) g_{01}^1(R) dR \right|^2 + J \left| \int_0^\infty S_n(R) j_{J-1}(KR) f_{vJ}^n(R) g_{01}^1(R) dR \right|^2. \quad (8)$$

If one neglects the coupling between vibrations and rotations, i.e., the dependence of f and g on J and J_i , then Eq. (8) is just a weighted average between $P_{nv(J+1)}$ and $P_{nv(J-1)}$ with $J_i=0$. We thus expect the main effect of an initial rotational excitation to be a ‘‘smearing’’ of the rotational distribution for $J_i=0$. The final-state distribution $P(E)$ for J_i

$=1$ is presented in the third column of Table III, where the zero of the excitation energy E_f has been shifted by the rotational excitation energy 4.96×10^{-3} eV of the initial T_2 molecule, to make the end-point energy consistent with that for $J_i=0$.

As seen from Table III a rotational excitation of the initial T_2 state will change not only the probabilities of different final rovibrational states but also transfer probability between the different electronic states. If we approximate the integral over R in Eq. (5) by the overlap of the electronic wavefunctions S_n evaluated at equilibrium nuclear separation R_e of the initial state [see Eq. (37) of Ref. [12]] it is easy to see how this happens. The rotational excitation will increase R_e somewhat, and through the R dependence of S_n (see Table II of Ref. [11]) the total transition probability of the electronic

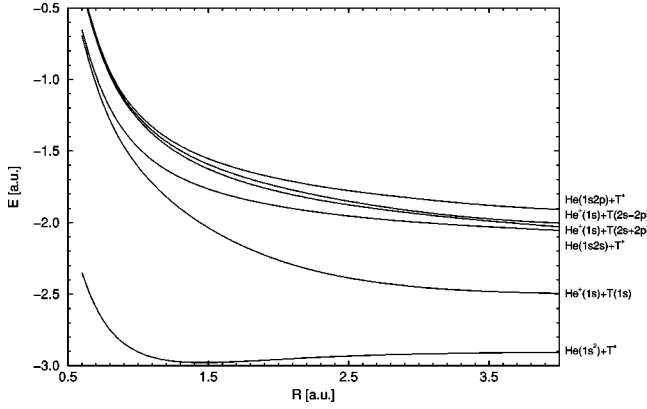


FIG. 1. Born-Oppenheimer potential energy curves for states 1–6, with dissociation limits indicated. The energies are taken from Table I, and interpolated using cubic splines. E is the electronic binding energy relative the total break-up threshold, R is the internuclear separation.

state will change accordingly. Since for $J_i=1$ the coupling between vibrations and rotations is small, R_e does not change much, and the resulting change in the integrated probability of the ground state is, according to Table III, only 0.018%. In Table IV we show how the effect increases for the first five rotationally excited states and for the lowest lying vibrationally excited states. The change in the total ground-state probability from rotational excitations is small ($\approx 0.1\%$), while a vibrational excitation would change the ground-state probability on the level of 1%. The ground-state probability varies almost linearly with the change in the average internuclear separation $\langle R \rangle$ of the rovibrational state. An elongation of the molecule of 0.04 a.u. would decrease the ground-state probability by about 1% (see Table IV).

C. Excited electronic states

Using the improved electronic wave functions and energies in Table I we have calculated the final-state probabilities also for the excited states. For the first time this has been done also for the TH isotope. The resulting transition prob-

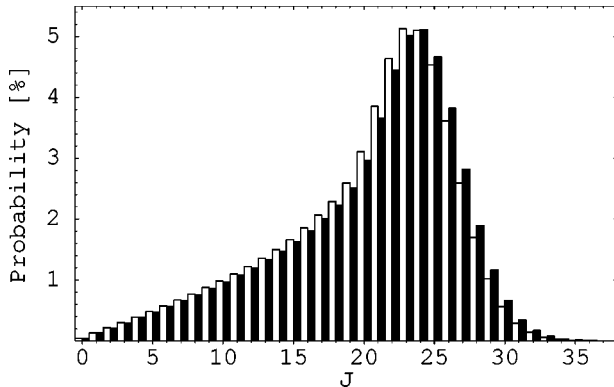


FIG. 2. The probability $P_{1J} = \sum_{\nu} P_{1\nu J}$ of rotational states J of the electronic ground state of ${}^3\text{HeT}^+$. The white bars show the results for a nonrelativistic and the black bars for a relativistic recoil momentum. The β -electron energy is $E_{\beta} = 18.6$ keV.

TABLE II. Transition probabilities $P_{1\nu J}$ (in %) to the rovibrational level with $J=23$ (for different vibrational states ν), without (nr) and with (r) the relativistic correction to the recoil momentum. The state $\nu=6$ is a predissociative resonance. The energy $E_{1\nu J}$ is in eV relative the state $\nu=J=0$.

ν	$E_{1\nu J}$	$P_{1\nu J}$ (nr)	$P_{1\nu J}$ (r)
0	1.08082	0.104	0.060
1	1.28153	0.614	0.470
2	1.46067	1.136	0.994
3	1.61740	1.175	1.128
4	1.75047	0.858	0.888
5	1.85797	0.500	0.552
6	1.93649	0.241	0.279

ability density for the most prominent states is shown in Fig. 3. All excited states are essentially dissociative (the potential curve of the first excited state has a shallow minimum at $R \approx 4.0$, which can be ignored, since it lies far outside the Franck-Condon region of the T_2 ground state) so the probability density is a continuous function of energy with peaks corresponding to the different excited states. Since its probability is very small, state 5 has not been included. The most important difference between the two isotopes is that the distribution for TH is shifted by about 1 eV towards lower energies. Since the upper limit on $m_{\nu}c^2$ approaches this value in the present experiments [2,3], it will be important to account for any impurity admixture of TH in the experimental analysis.

Above state 6 there exists an infinite number of Rydberg states, converging to the ionization threshold (i.e., the ground state of HeT^{++}). Although each of these states carries only a small transition probability, their added probability might be appreciable. It should, however, be noted that as long as the sudden approximation remains valid the condition that the total probability adds up to 1 is automatically fulfilled. This gives little room for the probability that can be carried by any additional components, as long as the transition probability to all other states remains unchanged.

In a calculation using a finite basis set it is of course not possible to determine all the Rydberg states. In our specific calculation seven additional bound states were found above state 6, which (together with state 5) have a total final-state probability 1.4%. Parts or all of them may be regarded as pseudo states, carrying the integrated final-state probability of the Rydberg states. We incorporated the effects of nuclear motion through the reflection approximation (which causes a broadening of the probability distribution similar to that for the states displayed in Fig. 3), and an effective energy shift due to recoil, as has been described in Ref. [19]. A more refined calculation could be made using quantum defect theory (as suggested in Ref. [29]). However, since their integrated probability is small, and since the nuclear motion has the effect of smoothing out all fine details, we judge our treatment to be sufficiently accurate.

D. Nonadiabatic effects

The form of the transition probability Eq. (5) was derived within the Born-Oppenheimer approximation. In this ap-

TABLE III. Dependence of the transition probability (as a function of excitation energy E_f of the final state) on the initial rotational state J_i of T_2 . Column 2 (3) contains the transition probability to the electronic ground state of ${}^3\text{HeT}^+$ for $J_i=0$ ($J_i=1$). Each entry $P_f(E_f)$ represents the integrated probability to the next higher energy in the table. The zero energy is located at the dissociation limit for ${}^3\text{HeT}^+$, 1.89741 eV above its rovibrational ground state.

E_f [eV]	$P_f(E_f)$ [%]	
	$J_i=0$	$J_i=1$
-1.90	0.007	0.008
-1.80	0.005	0.010
-1.70	0.023	0.026
-1.60	0.055	0.051
-1.50	0.046	0.080
-1.40	0.203	0.118
-1.30	0.165	0.268
-1.20	0.388	0.271
-1.10	0.381	0.571
-1.00	0.681	0.791
-0.90	1.121	1.041
-0.80	1.011	1.469
-0.70	2.441	2.367
-0.60	3.234	3.503
-0.50	4.086	4.575
-0.40	6.875	6.179
-0.30	6.628	5.889
-0.20	5.141	5.399
-0.10	6.556	6.093
0.00	5.459	4.931
0.10	3.723	3.711
0.20	2.547	2.737
0.30	1.696	1.927
0.40	1.137	1.337
0.50	1.695	1.917
0.75	1.009	1.013
1.00	0.573	0.569
1.25	0.281	0.289
1.50	0.132	0.137
1.75	0.062	0.064
2.00	0.042	0.043
2.50	0.008	0.008
3.00	0.002	0.002
Sum P_1 :	57.412	57.394

proximation the electronic part of the wave function is assumed to vary slowly with the internuclear distance R . Since the electronic overlap $S_n(R)$ does vary appreciably with R (see Table I and Ref. [8]), and since we are looking for small effects, it is worthwhile to investigate the validity of the Born-Oppenheimer approximation.

The corrections to the Born-Oppenheimer approximation arise mainly from the nuclear kinetic-energy operator acting on the electronic wave function. If the correction is small it can be evaluated in perturbation theory. In Ref. [20] we show that the first-order correction $P_{nvJ}^{(1)}$ to the transition probability to the rovibrational state v, J belonging to the

electronic state n of HeT^+ (described by the wave function Ψ_n) due to the nonadiabatic coupling to all other states n', v', J is

$$P_{nvJ}^{(1)} = 2 \text{Re} \left\{ \sum_{n'v'JM} \frac{1}{E_{nvJ} - E_{n'v'J}} \langle \Phi \xi_{000}^1 | e^{i\mathbf{K} \cdot \mathbf{R}} | \chi_{vJM}^n \Psi_n \rangle \right. \\ \times \int f_{vJ}^n(R) C_{nn'}(R) f_{v'J}^{n'}(R) dR \\ \left. \times \langle \Psi_{n'} \chi_{v'JM}^{n'} | e^{-i\mathbf{K} \cdot \mathbf{R}} | \Phi \xi_{000}^1 \rangle \right\}. \quad (9)$$

Here Φ is the wave function describing the electronic ground state of the initial T_2 molecule, and $C_{nn'}$ is the coupling between the electronic states

$$C_{nn'}(R) = -\frac{1}{2\mu} \left\langle \Psi_n \left| \frac{\partial^2}{\partial R^2} - \frac{1}{R^2} (L_x^2 + L_y^2) \right| \Psi_{n'} \right\rangle \\ - \frac{1}{\mu} \left\langle \Psi_n \left| \frac{\partial}{\partial R} \right| \Psi_{n'} \right\rangle \frac{\partial}{\partial R}. \quad (10)$$

In Eq. (10) μ is the reduced mass of the nuclei, and L_x, L_y are x, y components of the electronic angular momentum. A term proportional to $\mathbf{p}_1 \cdot \mathbf{p}_2$ has been neglected, where \mathbf{p}_i is the momentum operator of electron i .

The nonadiabatic Hamiltonian is invariant under rotations of the entire molecule. Therefore the rotational quantum number J is conserved. This is, however, not true for the electronic angular momentum Λ along the internuclear axis. Thus nonadiabatic couplings between $\Lambda=0$ and $\Lambda=1$, i.e., between Σ and Π states, do exist. Since the Σ - Π coupling is proportional to $\sqrt{J(J+1)}$ and $\langle J \rangle \approx 23$ one could expect it to be relatively large [30]. The corrections to the final-state probability due to the Σ - Π couplings do, however, vanish in first-order perturbation theory. The reason is that the last matrix element in Eq. (9) requires the electronic state n' to be of the same symmetry as the initial T_2 state, i.e., of Σ symmetry. Therefore couplings to Π states appear only in second-order perturbation theory, which is proportional to μ^{-2} and thus very small. It is therefore sufficient to consider nonadiabatic couplings only between Σ states.

In Ref. [20] we used an approximate sum rule to estimate $P_n^{(1)} = \sum_{vJ} P_{nvJ}^{(1)}$ for the ground state. The largest change in transition probability due to nonadiabatic couplings (about $7.4 \times 10^{-3}\%$) occurs in the coupling between the ground state and the first excited state. With the wave functions of nuclear motion f_{vJ}^n in hand we can calculate Eq. (9) without any simplifying approximation, using the couplings $C_{nn'}$ calculated in Ref. [20]. Since the excited states under consideration are dissociative, the summation over the vibrational quantum number v' in Eq. (9) goes over in an integral over E' , which designates the asymptotic translational energy of the dissociation fragments. Using the fact that $\int f_{vJ}^n(R) C_{nn'}(R) f_{v'J}^{n'}(R) dR = \int f_{v'J}^{n'}(R) C_{n'n}(R) f_{vJ}^n(R) dR$ to

TABLE IV. The integrated transition probabilities P_n to the electronic state n of ${}^3\text{HeT}^+$ for different initial rovibrational states (ν_i, J_i) of the T_2 molecule. $\langle R \rangle$ is the mean internuclear distance of T_2 in the given rovibrational state.

	$E_{\nu J}^{\text{T}_2}$ [eV]	$\langle R \rangle$ [a.u.]	P_1	P_2	P_3	P_4	P_6
$\nu_i=0, J_i=0$	-4.59093	1.42835	57.412	17.359	7.761	0.782	0.918
$\nu_i=0, J_i=1$	-4.58597	1.42907	57.393	17.373	7.758	0.782	0.918
$\nu_i=0, J_i=2$	-4.57605	1.43052	57.356	17.401	7.752	0.781	0.917
$\nu_i=0, J_i=3$	-4.56121	1.43268	57.299	17.444	7.744	0.780	0.916
$\nu_i=0, J_i=4$	-4.54149	1.43556	57.224	17.500	7.732	0.779	0.914
$\nu_i=0, J_i=5$	-4.51695	1.43915	57.130	17.570	7.718	0.777	0.913
$\nu_i=1, J_i=0$	-4.28535	1.48330	55.821	18.409	7.531	0.739	0.890
$\nu_i=2, J_i=0$	-3.98969	1.53947	54.204	19.483	7.298	0.698	0.864
$\nu_i=3, J_i=0$	-3.70379	1.59070	52.561	20.587	7.064	0.660	0.836
$\nu_i=4, J_i=0$	-3.42753	1.65602	50.891	21.725	6.828	0.624	0.809
$\nu_i=5, J_i=0$	-3.16081	1.71672	49.193	22.904	6.591	0.588	0.782

avoid taking the derivative of the rapidly oscillating wave function of nuclear motion for the excited state, Eq. (9) reduces to

$$\begin{aligned}
 P_{1\nu J}^{(1)} &= 2(2J+1) \int dE' \frac{1}{E_{n\nu J} - E'} \\
 &\times \int g_{00}^1(R) S_1(R) j_J(KR) f_{\nu J}^1(R) dR \\
 &\times \int f_J^2(E', R) C_{n'n}(R) f_{\nu J}^1(R) dR \int f_J^2(E', R) \\
 &\times S_2(R) j_J(KR) g_{00}^1(R) dR \quad (11)
 \end{aligned}$$

for couplings between the electronic ground state and the first excited one of HeT^+ . The results for $J=23$ are presented in Table V. We see that the relative change of the

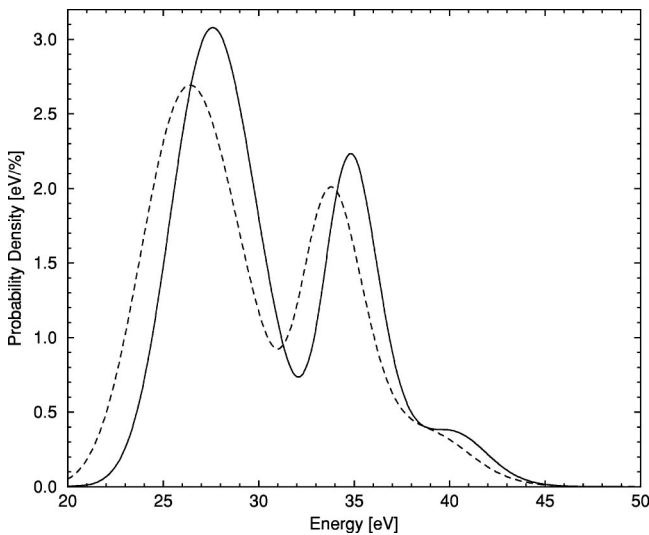


FIG. 3. The probability density for transitions to states 2, 3, 4, and 6 (see Table I), which are the dominating excited states below the ionization threshold. The solid curve is for ${}^3\text{HeT}^+$, the dashed one for ${}^3\text{HeH}^+$.

probability of each level is of the order of 10^{-3} or less. Translated into an absolute change of the integrated transition probability to the ground state this would correspond to about 0.06%. However, we see that in reality some rovibrational levels gain while others lose probability, the trend being to transfer probability to higher vibrational states. This causes a partial cancellation when the changes in probability of the individual rovibrational levels are added up to the total change in probability of the electronic ground state, making the one order of magnitude smaller estimate from the sum rule more likely. In any event, there is no evidence for a significant effect from nonadiabatic couplings. Therefore we have stopped short of a (very time-consuming) full calculation.

IV. PROSPECTS OF EXPERIMENTAL VERIFICATION OF THE FINAL STATE POPULATIONS

The excited states of the HeT^+ ion are of course not stable. Different modes of decay include dissociation, auto-ionization, and radiative deexcitation. Monitoring of the various decay yields may provide an independent check of the instantaneous populations of the HeT^+ states (i.e., immedi-

TABLE V. Transition probabilities (in %) to the bound and predissociative vibrational levels ν with rotational quantum number $J=23$. $P_{1\nu J}^{(0)}$ is the probability in the adiabatic approximation, while $P_{1\nu J}^{(1)}$ is the first-order correction due to the nonadiabatic coupling to the first excited state. The energy $E_{1\nu J}$ is in eV relative to the state $\nu=J=0$.

ν	$E_{1\nu J}$	$P_{1\nu J}^{(0)}$	$P_{1\nu J}^{(1)}$	$P_{1\nu J}^{(1)}/P_{1\nu J}^{(0)}$
0	1.08082	0.060	-9.6×10^{-5}	-1.6×10^{-3}
1	1.28153	0.470	-4.7×10^{-4}	-1.0×10^{-3}
2	1.46067	0.994	-5.5×10^{-4}	-5.5×10^{-4}
3	1.61740	1.128	-1.4×10^{-4}	-1.2×10^{-4}
4	1.75047	0.888	2.7×10^{-4}	3.0×10^{-4}
5	1.85797	0.552	3.9×10^{-4}	7.1×10^{-4}
6	1.93649	0.279	2.9×10^{-4}	1.0×10^{-3}

TABLE VI. Bound-bound rovibrational transition energies (in cm^{-1}) of the ${}^4\text{HeH}^+$ ground state. Experimental values are taken from the references in the last column, theoretical values have been obtained in this work.

$(v_i, J_i) \rightarrow (v_f, J_f)$	Experiment	Theory	Ref.
(0,10)→(0,11)	657.221	657.245	[41]
(0,11)→(0,12)	701.317	701.336	[41]
(0,12)→(0,13)	741.706	741.731	[41]
(0,13)→(0,14)	778.224	778.254	[41]
(0,14)→(0,15)	810.708	810.745	[41]
(0,15)→(0,16)	839.010	839.051	[41]
(0,16)→(0,17)	862.984	863.026	[41]
(0,17)→(0,18)	882.475	882.520	[41]
(0,18)→(0,19)	897.334	897.368	[41]
(0,20)→(0,21)	912.242	912.277	[41]
(0,21)→(0,22)	911.704	911.736	[41]
(1,10)→(1,11)	598.829	598.842	[41]
(1,11)→(1,12)	637.767	637.777	[41]
(1,12)→(1,13)	672.989	672.996	[41]
(1,13)→(1,14)	704.270	704.287	[41]
(1,14)→(1,15)	731.430	731.445	[41]
(1,15)→(1,16)	754.235	754.254	[41]
(1,16)→(1,17)	772.464	772.480	[41]
(1,17)→(1,18)	785.837	785.851	[41]
(1,18)→(1,19)	793.997	794.019	[41]
(1,19)→(1,20)	796.490	796.515	[41]
(1,20)→(1,21)	792.616	792.646	[41]
(2,13)→(2,14)	627.320	627.333	[41]
(2,14)→(2,15)	648.324	648.334	[41]
(2,15)→(2,16)	664.559	664.572	[41]
(2,16)→(2,17)	675.609	675.619	[41]
(2,17)→(2,18)	680.895	680.908	[41]
(2,18)→(2,19)	679.586	679.604	[41]
(2,19)→(2,20)	670.340	670.362	[41]
(0,1)→(1,0)	2843.9035	2844.237	[40]
(0,0)→(1,1)	2972.5732	2972.908	[40]
(0,2)→(1,1)	2771.8059	2772.134	[40]
(0,1)→(1,2)	3028.3750	3028.709	[40]
(0,3)→(1,2)	2695.0500	2695.375	[40]
(0,2)→(1,3)	3077.9919	3078.327	[40]
(0,4)→(1,3)	2614.0295	2614.351	[40]
(0,3)→(1,4)	3121.0765	3121.412	[40]
(0,4)→(1,5)	3157.2967	3157.630	[40]
(1,11)→(0,12)	1855.905	1856.153	[39]
(1,12)→(0,13)	1751.971	1752.199	[39]
(2,8)→(1,9)	1896.992	1897.143	[39]
(2,9)→(1,10)	1802.349	1802.500	[39]
(2,10)→(1,11)	1707.543	1705.692	[39]
(1,19)→(2,18)	862.529	862.633	[41]
(1,20)→(2,19)	745.624	745.721	[41]
(2,17)→(3,16)	833.640	833.743	[41]
(2,18)→(3,17)	719.769	719.870	[41]
(4,11)→(5,10)	901.963	902.056	[41]
(4,12)→(5,11)	807.806	807.909	[41]
(6,7)→(5,8)	863.378	863.451	[41]
(6,8)→(5,9)	782.925	782.993	[41]
(7,3)→(6,4)	817.337	817.423	[41]
(7,4)→(6,5)	760.259	760.484	[41]

ately after the β decay). In the following we will review some of the possibilities, using the results from the preceding sections.

In this context it is important to remember that the neutrino mass is determined only from the very small fraction of decays resulting in a β electron with an energy close to the maximum 18.6 keV. This is where the β -electron spectrum is sensitive to the neutrino mass, as was explained in Sec. II. However, an independent check of the final-state populations might involve an experiment which samples β electrons of *all* energies. Since the average β -electron kinetic energy is much smaller than the end-point energy, the average of any quantity that depends on the recoil, e.g., the population of the rovibrational levels, will differ significantly from its value at the end point of the β -electron spectrum.

The transition probability to a particular electronic state is on the other hand, within the sudden approximation, independent of the recoil momentum, as is evident from the sum-rule considerations (see Sec. III A). Thus, provided that the sudden approximation still holds [18,19], and that the contribution from the exchange between the β electron and the molecular electrons is still negligible, the large-scale features of the molecular final-state populations (on the level of electronic states) should not depend on the kinetic energy of the β electron. To test finer details, arising from the distribution of rovibrational levels one could make a coincidence measurement selecting only those decays resulting in a β -electron energy close to its maximum value. Such a selection would however reduce the statistics drastically (as is the case in neutrino-mass experiments), as well as introduce additional experimental complications.

Alternatively calculations for all different β -electron energies could be made. One must, however, remember that Eq. (9) was derived under the assumptions that the sudden approximation holds, and that the exchange contribution as well as the momentum of the neutrino can be neglected. For sufficiently low β -electron energies all of these conditions will fail. Comparison between an experiment and the results of such a calculation would therefore not be a *direct* test of the final-state distribution used in the neutrino-mass determination, but would of course still be a valuable check of the theory.

A. Mass spectrometry

Early attempts were made to determine the dissociation probability of the ${}^3\text{HeT}^+$ molecule through mass spectrometry of the fragments [31,32]. After the β decay the daughter molecule may either remain bound, or it may dissociate. If the final decay product is a molecular or atomic ion it can be identified through mass spectrometry (because of the nearly equal masses, T^+ ions and ${}^3\text{He}^+$ ions may however be difficult to discriminate). Since the mode of dissociation is different for different electronic states, the yields of the various dissociation products can give some information on the relative populations of the electronic states after the β decay. It is, however, important to know that the dissociation products really originate from the final state of the β decay, and not from some secondary process such as dissociation of

TABLE VII. Bound to quasibound, and quasibound to quasibound rovibrational transition energies E , and widths Γ of the upper quasibound state, for the ground state of various HeH^+ isotopes. Experimental values are taken from the references in the last column, theoretical values have been obtained in this work. Transitions marked by asterisk are quasibound to quasibound, for which the width refers to the upper level. (All quantities in cm^{-1} .)

isotope	$(v_i, J_i) \rightarrow (v_f, J_f)$	E (experiment)	E (theory)	Γ (experiment)	Γ (theory)	Ref.
$^4\text{HeH}^+$	$(5,12) \rightarrow (6,13)$	979.904	980.011	0.103	0.107	[42]
$^4\text{HeH}^+$	$(5,12) \rightarrow (7,11)$	938.2	937.865	4.1	3.9	[42]
$^4\text{HeH}^+$	$(0,23) \rightarrow (0,24)$	891.888	891.920		≈ 0	[43]
$^4\text{HeH}^+$	$(0,24) \rightarrow (0,25)^*$	870.298	870.331		4.3×10^{-7}	[43]
$^4\text{HeH}^+$	$(0,25) \rightarrow (0,26)^*$	837.180	837.213	0.0189	0.019	[43]
$^4\text{HeH}^+$	$(1,21) \rightarrow (1,22)$	781.245	781.288		≈ 0	[43]
$^4\text{HeH}^+$	$(1,22) \rightarrow (1,23)^*$	760.232	760.376		5.4×10^{-7}	[43]
$^4\text{HeH}^+$	$(1,23) \rightarrow (1,24)^*$	724.933	724.978	0.092	0.070	[43]
$^4\text{HeH}^+$	$(2,20) \rightarrow (2,21)$	650.613	650.645		6.2×10^{-7}	[43]
$^4\text{HeD}^+$	$(5,20) \rightarrow (7,19)$	944.720	944.895	1.8×10^{-2}	1.6×10^{-2}	[42]
$^4\text{HeD}^+$	$(5,20) \rightarrow (6,21)$	1003.329	1003.425	1.0×10^{-3}	4.4×10^{-4}	[42]
$^4\text{HeD}^+$	$(4,22) \rightarrow (6,21)$	1088.373	1088.552	8.1×10^{-4}	4.4×10^{-4}	[42]
$^4\text{HeD}^+$	$(9,4) \rightarrow (13,5)$	1073.475	1073.330	2.7×10^{-2}	4.5×10^{-2}	[42]
$^4\text{HeD}^+$	$(9,6) \rightarrow (13,5)$	911.705	911.398	2.7×10^{-2}	4.5×10^{-2}	[42]
$^3\text{HeH}^+$	$(5,11) \rightarrow (6,12)$	981.322	981.404	2.9×10^{-2}	3.2×10^{-2}	[42]
$^3\text{HeD}^+$	$(5,18) \rightarrow (6,19)$	1034.144	1034.174	4.5×10^{-4}	4.1×10^{-5}	[42]
$^3\text{HeD}^+$	$(5,18) \rightarrow (7,17)$	995.415	995.458	5.6×10^{-3}	4.3×10^{-3}	[42]

other T_2 or $^3\text{HeT}^+$ molecules due to collisions with fast β electrons. In addition, the experiment has to be performed in such a way that recombination of the ions is prevented.

There are five different possibilities for the final $^3\text{HeT}^+$ molecule. It may dissociate into $^3\text{He}^+ + \text{T}$, into $^3\text{He} + \text{T}^+$, or it may remain bound. Above the threshold for (double) ionization of HeT^+ one may also have dissociation into $^3\text{He}^+ + \text{T}^+$, and even into $^3\text{He}^{++} + \text{T}$.

The first case, dissociation into $^3\text{He}^+ + \text{T}$, will be the fate of molecules ending up in electronic states 2, 4, and 5 (see Fig. 1), in the Rydberg states [which in the asymptotic limit converge to $\text{He}^+(1s) + \text{T}^+$, into which the ground state of HeT^{++} dissociates, see Sec. III C] as well as in the dominating resonances above the ionization threshold. The three electronically bound states and the Rydberg states add up to about 19.5% of the final-state probability. This number does not depend on the kinetic energy of the β electron because the states have no minima in the relevant R region, and will therefore always dissociate, regardless of the magnitude of the recoil. The additional contribution from the resonances is difficult to determine exactly, since here dissociation competes with ionization which occurs on the same time scale ($\approx 10^{-15}$ s), an upper limit being thus the integrated probability of the resonances, about 8%. If ionization occurs before the nuclei have been separated enough to stabilize the molecule against this process, the dissociation fragments will instead be $^3\text{He}^+$ and T^+ (since the resonances are located under the threshold for double ionization of He). Thus when the autoionizing resonances dissociate one $^3\text{He}^+$ ion will be produced with certainty, and in some cases also a T^+ ion.

The second type of dissociation, $^3\text{He} + \text{T}^+$, will follow all decays to state 3 and 6, and after decay to the dissociative

part of the ground state (see Fig. 1). State 3 and 6 make up 8.7% of the final-state probability, while the dissociation probability of the ground states depends on the recoil, i.e., on the energy of the β electron. When the energy of the β electron is close to its maximum there will be 18.4% probability for decay into the dissociative region of the electronic ground state, and 39.0% probability that the ground state remains bound. Thus in total, at the end-point energy of the β electron, there is 27.1% probability that the final state dissociates to $^3\text{He} + \text{T}^+$. Since the average recoil is smaller than the recoil at the end point this value can be taken as an upper bound for the probability of this mode of dissociation. A corresponding lower bound can be obtained by assuming that the ground state never dissociates. For decay of TH the electronic ground state has only a small probability to dissociate (about 1.5% at the end point), so the probability for $\text{H}^+ + ^3\text{He}$ dissociation should be close to this lower limit, i.e., 8.7%.

Within the nonresonant part of the electronic continuum the ionization will be much faster than the nuclear motion, and for lower energies (less than 80 eV) the dissociation channel will be $^3\text{He}^+ + \text{T}^+$. At higher energies the two channels $^3\text{He}^+ + \text{T}^+$, and $^3\text{He}^{++} + \text{T}$ will compete. Their relative probabilities will depend on the corresponding probabilities for the various $^3\text{HeT}^{++}$ states (all dissociative within the Franck-Condon region for T_2 [33]) to be the final state of the ionization process. The integrated final-state probability of this part of the electronic continuum is about 6%, about 4% of which lies below 80 eV [19].

All in all we then expect between 0.31 and 0.34 $^3\text{He}^+$ ions per β decay, 0.13 to 0.41 T^+ ions per decay, 0.39 to 0.57 $^3\text{HeT}^+$ ions per decay, and a small number (0 to 0.02

per decay) of ${}^3\text{He}^{++}$ ions, when considering *all* β decays. Since at least some decays will result in dissociation to ${}^3\text{He}^+ + \text{T}^+$, i.e., *two* ions, the sum of all ${}^3\text{He}^+$, T^+ , ${}^3\text{HeT}^+$, and ${}^3\text{He}^{++}$ per decay should actually be slightly larger than 1. If the ${}^3\text{He}^+$ ions and T^+ cannot be discriminated they add up to a single component of 0.44 to 0.75 ions per decay. Depending on experimental conditions it may be advantageous to either measure absolute yields, or the appropriate ratios between the yields of different ions. For the decays resulting in β -electron energies close to its maximum value we expect 0.31 to 0.34 ${}^3\text{He}^+$ ions, 0.31 to 0.41 T^+ ions, and 0.39 ${}^3\text{HeT}^+$ ions per β decay.

In the late 1950s a couple of mass-spectrometry experiments were done, the results of which are in sharp disagreement with the theoretical predictions given above. Wexler *et al.* measured the probability that the daughter ion remains bound after β decay of T_2 to be $94.5 \pm 0.6\%$, and after decay of TH $89.5 \pm 1.1\%$ [32]. Snell *et al.* measured TH and obtained $93.2 \pm 1.9\%$ probability that the daughter ion remains bound [31]. A possible reason for this disagreement was however given by Wexler [32]. The mass spectrometers used “strongly discriminate against ions with appreciable translational energy.” Since the translational energies of the dissociation fragments from the excited states are 8 to 26 eV, and from the ground state 0 to 3 eV, we find this explanation plausible. Recombination during the transit to the spectrometer is also a potential source of errors. It would be very interesting to see these experiments repeated with modern technology.

B. Photon yields

Another mode of deexcitation is *via* emitting a photon. The different excited states can be identified by the wavelength of the photons, and the yields at different wavelengths provide information regarding the populations of the different excited states, i.e., the final-state probability of the excited state.

It is of course important to allot for other modes of deexcitation, such as collisions with other molecules. One must also be careful to separate *secondary* excitations due to the β electron passing through the source or due to other collisional processes. Schmieder has measured the optical spectrum of T_2 gas in the wavelength region 350–800 nm [34]. A large number of transitions were observed, almost all of them originating from secondary excitations. Only one primary transition was observed, ${}^3\text{He}^+(n=4 \rightarrow n=3)$. The same transition was observed by Wexler and Porter [35].

Which other radiative transitions could then be observed? If we first concentrate on transitions between electronic states there will obviously be no transitions from the ground state. The excited states are all dissociative, with a typical dissociation of the order of 10^{-15} s. The typical time for radiative transitions can be estimated by comparing to the times for atomic hydrogen and helium, which yields a typical time of 10^{-10} s or more. Thus radiative processes are slow compared to dissociation. Therefore, we expect that only photons from deexcitations of the dissociation fragments can be observed. State 2 dissociates to the atomic ground states

$\text{He}^+(1s) + \text{T}(1s)$, which will not be possible to observe. State 3 dissociates to $\text{He}(1s2s) + \text{T}^+$, which according to the $\Delta l = \pm 1$ selection rule only can be deexcited through a two photon transition, which is a very slow process, and it is therefore very likely that deexcitation *via* collision occurs.

Thus we are left with states 4, 5, and 6, which make up less than 2% of the total transition probability, and the states above the ionization limit, which add up to about 14%. Since these states are very close in energy one can expect avoided crossings between the potential curves as the nuclear separation R is increased (see Fig. 1). This leads to large couplings between the states, which makes it extremely demanding to calculate the exact probabilities for different dissociation channels ($\text{He}^+ + \text{T}$ versus $\text{He} + \text{T}^+$, and/or different excitations of atomic states) from a given population of the various electronic states around $R = 1.4$ a.u. For the resonances there is of course the additional complication of the competing ionization channel. Therefore the calculation required to make this prediction will in fact be more difficult than the original calculation of the final-state probabilities just after the β decay that we want to verify.

It is also possible to study the infrared light emitted in transitions between the rovibrational levels of the ground state. In fact one such experiment has been made, where the $\nu=1 \rightarrow \nu=0$ transition has been detected [36]. For these states there is no problem with dissociation, but once again one must remember that the population probability to a specific rovibrational state is recoil dependent, and thus different if the entire β spectrum is integrated over, or if, as in neutrino-mass experiments, only decays resulting in a β -electron energy close to the end point are selected (see the discussion in the beginning of this section). The life times of these states are expected to be long, of the order of milliseconds [37]. Radiative deexcitation will therefore compete with collisional deexcitations and with recombination through the capture of a free electron.

C. Experiments on HeH^+

While the experiments described above aim at a direct verification of the instantaneous final-state populations following the β decay of T_2 , it is also possible to test the theory for the HeH^+ molecule by measurements of other properties of this molecule. The disadvantage of these methods is of course that the part of the theory relating directly to the β -decay process is not tested. Experimentally this is however an advantage, since the experiments do not have to use radioactive tritium, but can just as well use other isotopes that are harmless and easier accessible, e.g., ${}^4\text{HeH}^+$.

Even though the calculation of the matrix elements in Eq. (6) can only be tested in decay experiments, the accuracy of the HeH^+ wave functions can be tested in experiments involving other ways of populating the HeH^+ states to be tested. For example, photoabsorption experiments could be performed on HeH^+ . This process would produce excited states in a way similar to that of β decay (although with a different probability distribution). The theoretical predictions for the subsequent dissociation process could then be checked experimentally using, e.g., the methods described in

Secs. IV A and IV B, but with the advantage of allowing a selective probing of a certain final-state energy region. This could, e.g., allow for testing the rovibrational shapes of the electronic states, without complications arising from the recoil. Such theoretical predictions have been made in Ref. [38].

Some experiments have been done on radiative transitions between ground-state rovibrational levels in HeH^+ . These experiments can be used to verify the calculations of the energy spectrum of HeH^+ , but give no information on transition probabilities. Still they provide some consistency check of the calculations.

Tolliver, Kyrala, and Wing [39], Bernath and Amano [40], and Liu and Davies [41] have measured a large number of bound-bound rotational and rovibrational transitions in the electronic ground state of $^4\text{HeH}^+$. In Table VI their results are compared to our theoretical calculations, using the methods described above in Sec. III. We find that the difference between experiment and theory is less than $1 \text{ cm}^{-1} \approx 10^{-4} \text{ eV}$, a precision that certainly is more than sufficient for the neutrino-mass experiments. Carrington *et al.* [42], and Lie and Davies [43] have also measured some transitions involving predissociative resonances of the electronic ground state. The predissociative resonances are sensitive to the long range part of the potential curve, and are therefore more difficult to calculate accurately. In neutrino-mass experiments only the R region within the Franck-Condon region of the T_2 ground state (i.e., $R < 4 \text{ a.u.}$) is important. The results in Table VII show that the calculated energies agree with experiment within 1 cm^{-1} . We have also calculated the widths of the predissociative resonances, using the program LEVEL6.0 by Le Roy [27]. In this program the widths of predissociative resonances are calculated using a semiclassical method with Airy-function boundary condition, described in Refs. [44–46]. We see that for the wider resonances the agreement between theory and experiment is rather good, while for the narrower resonances there is a discrepancy. The exact widths of the resonances are, however, of no importance for the neutrino-mass determination.

V. CONCLUSIONS

We have refined the bound-state part of the HeT^+ final-state spectrum following the β decay of T_2 by including the relativistic correction to the recoil, and by using improved potential energy curves for the excited states. The calcula-

tions have been performed for decay of both T_2 and TH, to allow for interpretation of experiments with TH admixture. The change in the final-state spectrum due to rotational excitations of the initial T_2 molecules has been evaluated, and found to be proportional to the elongation of the T_2 molecule. Nonadiabatic corrections to the Born-Oppenheimer approximation have been investigated and found negligible.

There are various ways by which the theoretical final-state spectrum could be tested in experiments. Direct methods would be either to identify the dissociation fragments from the HeT^+ molecule by mass spectrometry, or to measure the photons emitted when excited final states decay. In practice, due to the short dissociation times, also the latter method would in fact be a measurement of the dissociation fragments. It turns out that it is very difficult to devise an experiment that tests exactly the final-state spectrum that is used for neutrino-mass determination. In most cases predictions of the quantities that could actually be measured require theoretical calculations that appear to be more difficult and thus necessarily less accurate than the calculations needed for the determination of the instantaneous final-state populations used for neutrino-mass determination.

Alternatively one may test the accuracy of the molecular part of the theory via other types of experiments on HeH^+ . Although the information from such experiments would not relate directly to the β -decay process, they would on the other hand still be useful, and probably be easier to perform and interpret.

The available experimental data on rovibrational levels of HeH^+ isotopes have been compared to theoretical results from our calculations. The agreement was in most cases found to be very good, confirming the validity of the theoretical and numerical apparatus applied.

ACKNOWLEDGMENTS

This work was partially supported by the National Science Foundation through a grant for the Institute for Theoretical Atomic and Molecular Physics at Harvard University and Smithsonian Astrophysical Observatory, where parts of this work were carried out. The authors also gratefully acknowledge the bilateral support from the Swedish Institute and the Deutscher Akademischer Austauschdienst. This work was also supported from the Swedish Natural Science Research Council (NFR).

-
- [1] Y. Fukuda *et al.*, Phys. Rev. Lett. **81**, 1562 (1998).
 - [2] H. Barth *et al.*, Prog. Part. Nucl. Phys. **40**, 353 (1998).
 - [3] V. M. Lobashev, Prog. Part. Nucl. Phys. **40**, 337 (1998).
 - [4] R. G. H. Robertson *et al.*, Phys. Rev. Lett. **67**, 957 (1991).
 - [5] Ch. Weinheimer *et al.*, Phys. Lett. B **300**, 210 (1993).
 - [6] W. Stoefl and D. J. Decman, Phys. Rev. Lett. **75**, 3237 (1995).
 - [7] A. I. Belevsev *et al.*, Phys. Lett. B **350**, 263 (1995).
 - [8] W. Kołos, B. Jeziorski, K. Szalewicz, and H. J. Monkhorst, Phys. Rev. A **31**, 551 (1985).
 - [9] B. Jeziorski *et al.*, Phys. Rev. A **32**, 2573 (1985).
 - [10] O. Fackler *et al.*, Phys. Rev. Lett. **55**, 1388 (1985).
 - [11] W. Kołos, B. Jeziorski, H. J. Monkhorst, and K. Szalewicz, Int. J. Quantum Chem., Symp. **19**, 421 (1986).
 - [12] K. Szalewicz *et al.*, Phys. Rev. A **35**, 965 (1987).
 - [13] W. Kołos *et al.*, Phys. Rev. A **37**, 2297 (1988).
 - [14] P. Froelich *et al.*, J. Phys. B **20**, 6173 (1987).
 - [15] P. Froelich *et al.*, Phys. Rev. Lett. **71**, 2871 (1993).
 - [16] S. Jonsell and H. J. Monkhorst, Phys. Rev. Lett. **76**, 4476 (1996).
 - [17] P. Froelich and A. Saenz, Phys. Rev. Lett. **77**, 4724 (1996).

- [18] A. Saenz and P. Froelich, Phys. Rev. C **56**, 2132 (1997).
[19] A. Saenz and P. Froelich, Phys. Rev. C **56**, 2162 (1997).
[20] S. Jonsell, A. Saenz, and P. Froelich, Pol. J. Chem. **72**, 1323 (1998).
[21] A. Saenz, S. Jonsell, and P. Froelich, Phys. Rev. Lett. (submitted).
[22] W. Kołos, K. Szalewicz, and H. J. Monkhorst, J. Chem. Phys. **84**, 3278 (1986).
[23] W. Kołos, Int. J. Quantum Chem. **10**, 217 (1976).
[24] W. Kołos and J. M. Peek, Chem. Phys. **12**, 381 (1976).
[25] D. M. Bishop and L. M. Cheung, J. Mol. Spectrosc. **75**, 462 (1979).
[26] W. Kołos and L. Wolniewicz, J. Chem. Phys. **43**, 2429 (1965).
[27] R. J. Le Roy, Report No. CP-555, University of Waterloo, Ontario, Canada.
[28] R. J. Le Roy, Comput. Phys. Commun. **52**, 383 (1989).
[29] J. Tennyson, J. Phys. B **31**, L177 (1998).
[30] W. Kołos and L. Wolniewicz, Rev. Mod. Phys. **35**, 473 (1963).
[31] A. H. Snell, F. Pleasonton, and H. E. Leming, J. Inorg. Nucl. Chem. **5**, 112 (1957).
[32] S. Wexler, J. Inorg. Nucl. Chem. **10**, 8 (1959).
[33] T. G. Winter, M. D. Duncan, and N. F. Lane, J. Phys. B **10**, 285 (1977).
[34] R. W. Schmieder, J. Opt. Soc. Am. **72**, 593 (1982).
[35] S. Wexler and F. T. Porter, J. Chem. Phys. **50**, 5428 (1969).
[36] R. Raitz von Frenzt, K. Luchner, H. Micklitz, and V. Wittwer, Phys. Lett. **47A**, 301 (1974).
[37] S. Datz and M. Larsson, Phys. Scr. **46**, 343 (1992).
[38] A. Saenz and P. Froelich (in preparation).
[39] D. E. Tolliver, G. A. Kyrala, and W. H. Wing, Phys. Rev. Lett. **43**, 1719 (1979).
[40] P. Bernath and T. Amano, Phys. Rev. Lett. **48**, 20 (1981).
[41] Z. Liu and P. B. Davies, J. Chem. Phys. **107**, 337 (1997).
[42] A. Carrington *et al.*, Chem. Phys. **81**, 251 (1983).
[43] Z. Liu and P. B. Davies, Phys. Rev. Lett. **79**, 2779 (1997).
[44] R. J. Le Roy and R. B. Bernstein, J. Chem. Phys. **54**, 5114 (1971).
[45] R. J. Le Roy and W. K. Liu, J. Chem. Phys. **69**, 3622 (1978).
[46] J. N. L. Connor and A. D. Smith, Mol. Phys. **43**, 397 (1981).